How to cite: *Angew. Chem. Int. Ed.* **2024**, *63*, e202401486
doi.org/10.1002/anie.202401486

Nucleic Acids

Universal crRNA Acylation Strategy for Robust Photo-Initiated One-Pot CRISPR–Cas12a Nucleic Acid Diagnostics

Pengfei Liu[+], Yating Lin[+], Xiaohua Zhuo[+], Jiayu Zeng, Bolin Chen, Zhen Zou, Guhuan Liu, Erhu Xiong, and Ronghua Yang**

Abstract: Spatiotemporal regulation of clustered regularly interspaced short palindromic repeats (CRISPR) system is attractive for precise gene editing and accurate molecular diagnosis. Although many efforts have been made, versatile and efficient strategies to control CRISPR system are still desirable. Here, we proposed a universal and accessible acylation strategy to regulate the CRISPR–Cas12a system by efficient acylation of 2′-hydroxyls (2′-OH) on crRNA strand with photolabile agents (PLGs). The introduction of PLGs confers efficient suppression of crRNA function and rapid restoration of CRISPR–Cas12a reaction upon short light exposure regardless of crRNA sequences. Based on this strategy, we constructed a universal PhotO-Initiated CRISPR–Cas12a system for Robust One-pot Testing (POIROT) platform integrated with recombinase polymerase amplification (RPA), which showed two orders of magnitude more sensitive than the conventional one-step assay and comparable to the two-step assay. For clinical sample testing, POIROT achieved high-efficiency detection performance comparable to the gold-standard quantitative PCR (qPCR) in sensitivity and specificity, but faster than the qPCR method. Overall, we believe the proposed strategy will promote the development of many other universal photo-controlled CRISPR technologies for one-pot assay, and even expand applications in the fields of controllable CRISPR-based genomic editing, disease therapy, and cell imaging.

[*] P. Liu,[+] Y. Lin,[+] X. Zhuo,[+] J. Zeng, Dr. Z. Zou, Prof. G. Liu, Prof. E. Xiong, Prof. R. Yang
Key Laboratory of Chemical Biology & Traditional Chinese Medicine Research, Ministry of Education
College of Chemistry and Chemical Engineering
Hunan Normal University
410081 Changsha, P. R. China
E-mail: xiongerhu2008@163.com
Yangrh@pku.edu.cn

Dr. B. Chen
The Second Department of Thoracic Oncology, Hunan Cancer Hospital & The Affiliated Cancer Hospital of Xiangya School of Medicine
Central South University
410013 Changsha, P. R. China

[+] These authors contributed equally to this work.

Introduction

Clustered regularly interspaced short palindromic repeats (CRISPR) systems are a fundamental part of the prokaryotic adaptive immune systems against invasive nucleic acids by means of guide RNA (gRNA) or CRISPR RNA (crRNA)-guided, complementarity-dependent CRISPR recognition and cleavage event.[1,2] Due to high specificity and crRNA programmability, CRISPR technology has been rapidly repurposed for various biotechnological and molecular applications, including gene editing,[3,4] gene imaging,[5,6] cellular events recording,[7] and molecular diagnostics.[8–11] Among CRISPR systems, some Cas effectors, such as Cas12 and Cas13, not only present highly precise target recognition and site-specific target cleavage activity (*cis*-cleavage), but also unleash high-efficiency non-specific single-stranded DNA or RNA cleavage (*trans*-cleavage) activity.[12–15] Benefited from these eminent properties, a series of CRISPR-based diagnostics platform, such as DETECTR (DNA endonuclease-targeted CRISPR trans reporter),[13] HOLMES (one-HOur Low-cost Multipurpose highly Efficient System),[16] SHERLOCK (Specific High-Sensitivity Enzymatic Reporter UnLOCKing),[17] and so forth, have been exploited for the sensitive and specific detection of DNA and RNA by incorporating with isothermal nucleic acid amplification or polymerase chain reaction (PCR), as well as a fluorogenic probe as an alternative actuating process to generate detectable output signals. However, these CRISPR-based detection approaches require a two-step process, that is, separating target preamplification and CRISPR-mediated signal readout steps. The two-step detection process involves multi-step manual operations, undoubtedly, making the detection workflow complicated and turnaround time extended. In addition, usually in the transfer process, only a portion of amplification products is used in the subsequent CRISPR detection, and most of the amplification products are not effectively utilized, which artificially reduces the efficiency of nucleic acid amplification and causes the distortion of detection signals. Especially for the low-concentration target, it may not be detected, resulting in false negative results. More importantly, multiple liquid-handling steps potentially increase the risk of aerosol contaminations and consequently generate false positive results.[18–20] It was recently demonstrated that it is possible to simply integrate isothermal amplification with CRISPR system into one-step reaction.[18,21–23] However, a major obstacle is the low reaction compatibility of isothermal amplification and CRISPR system in the one-step

© 2024 Wiley-VCH GmbH

detection, because once the CRISPR system is activated, its potent cleavage will inevitably destruct nucleic acid amplification templates (amplicons) and primers, thus leading to a low amplification efficiency and detection sensitivity. To address this issue, several researchers have done some attempts such as physically isolating reaction reagents,[24–27] using phase separation solutions,[28,29] or employing suboptimal protospacer adjacent motif (PAM).[19] Despite the progress, these strategies still are inconvenient or sacrifice the efficacy of the CRISPR reaction.

Light represents an excellent remote regulation element since irradiation can be easily controlled in a spatial and temporal fashion.[30] To date, photo-controlled CRISPR–Cas9 systems have been widely developed to realize precise control over gene manipulation.[31–36] Inspired by these studies, recently, Zhou and Liu et al. creatively introduced photo-controlled technology into one-pot CRISPR assay to separate the isothermal amplification and CRISPR detection in the time dimension, thus ensuring high detection efficiency.[37–39] In these works, the crRNA was blocked by photocleavable linker (PC linker)-modified complementary oligonucleotide or photosensitive 6-nitropiperonyloxymethyl (NPOM)-caged thymidine base, which was used to temporarily suppress the CRISPR–Cas12a activity. In such case, the inactive Cas12a system would not interfere with nucleic acid amplification. When the amplification reaction is complete, the CRISPR–Cas12a activity would be restored rapidly upon light irradiation, followed by Cas12a-mediated recognition, cleavage and signal readout, thus realizing a one-pot, high-efficiency nucleic acid detection. Despite current approaches with great promise, the low universality makes them less than ideal because the position and number of PC linker or NPOM require cumbersome trial-and-error screening according to the changes of target sequence.[40,41] Therefore, a versatile strategy that does not perform permutation and combination screening of modifications, regardless of target sequences, but can rapidly restore the CRISPR–Cas12a activity upon exposure to light irradiation, is still desirable for photo-initiated one-pot CRISPR assay.

2′-hydroxyl (2′-OH) is a characteristic functional group in RNA ribose, regardless of sequence, and reactions involving 2′-OH group are in principle the most generalized pattern for covalent modification of RNA.[42] Recent studies demonstrated that RNA structure and function could be destroyed by 2′-OH group acylation (‘cloaking’) using acylimidazole reagents, and efficiently reinstated with a removal of acylation adducts (‘uncloaking’) upon the external addition of chemical reagents, representing a promising strategy for external control over the function of RNA and gRNA in CRISPR systems.[43–50] It is conceivable that the gRNA function can be temporarily suspended by attaching photolabile groups (PLGs) on 2′-OH group, and subsequently restored by light irradiation. In view of this, Zhou and Tian group adopted RNA 2′-OH acylation to develop photo-controlled CRISPR–Cas9 system for genome editing in human cells.[51] While we envisioned that the acylation strategy will also benefit the development of versatile photo-initiated one-pot CRISPR assay due to independence on crRNA or target sequence. However, to the best of our knowledge, the exploration of such an excellent acylation strategy in the field of one-pot CRISPR assay has not been reported.

In this work, we developed a universal strategy that can gain photocontrol over crRNAs by rapid 2′-OH acylation with PLGs. To this end, we first synthesized a photocloaking agent, which showed a high-yield reaction with 2′-OH group on crRNA strand, affording efficient inhibition of CRISPR–Cas12a activity, regardless of crRNA sequences. As expectedly, the light irradiation could effectively remove these PLG adducts and reinstate the CRISPR–Cas12a activity. Based on the photoresponsive cloaked crRNA, we integrated the *trans*-cleavage effect of Cas12a with recombinase polymerase amplification (RPA) to establish a rapid nucleic acid detection platform, termed POIROT (PhotO-Initiated CRISPR–Cas12a system for Robust One-pot Testing). POIROT ensures that all components are added to a closed, single-tube system and thus avoids the risk of aerosol contamination. Due to the sequential execution of RPA and CRISPR–Cas12a reaction, they do not interfere with each other, achieving relatively high detection efficiency. It is demonstrated that POIROT is about two orders of magnitude more sensitive than the conventional one-step assay and comparable to the two-step assay. For clinical sample testing, POIROT achieved high-efficiency detection comparable to the gold-standard quantitative PCR (qPCR) in sensitivity and specificity, but faster than the qPCR method. Additionally, POIROT based on photoresponsive cloaked crRNA is easily extend to other CRISPR systems, such as CRISPR–Cas13 and CRISPR–Cas14 systems, for one-pot nucleic acid assay. We anticipated this approach will contribute to the development of universal and accessible photo-controlled CRISPR technologies, highlighting their potentials in genomic editing, disease therapy, and cell imaging.

Results and Discussion

One-Step Cloaking and Photo-Induced Uncloaking of crRNA

The aim of this work is to develop a universal approach that can gain photocontrol over crRNAs by 2′-OH acylation with photocloaking agent to regulate CRISPR–Cas12a system. To this end, we synthesized the photocloaking agent (Figure 1a) and characterized by ^{1}H NMR (Figure S1 and S2). We anticipated that the 2′-OH group of crRNA strand can be temporarily cloaked by attaching PLG adducts, and subsequently reinstated after light-triggered removal of PLG adducts (Figure 1b). We thus estimated the attaching PLGs on 2′-OH group of crRNA strand via an acylation reaction. As a proof-of-concept, a randomly designed crRNA strand was used to perform cloaking experiment (Table S1). After one-step mild reaction and simple post-treatment procedures, the cloaked crRNA was obtained, followed by characterized using polyacrylamide gel electrophoresis (PAGE). As expected, we observed new higher mobility-shifted bands with the prolonging time of acylation reaction, signifying continuously incremental PLG adducts

© 2024 Wiley-VCH GmbH

15213773, 2024, 23, Downloaded from https://onlinelibrary.wiley.com/doi/10.1002/anie.202401486 by Shanghai Normal University, Wiley Online Library on [09/04/2025]. See the Terms and Conditions (https://onlinelibrary.wiley.com/terms-and-conditions) on Wiley Online Library for rules of use; OA articles are governed by the applicable Creative Commons License

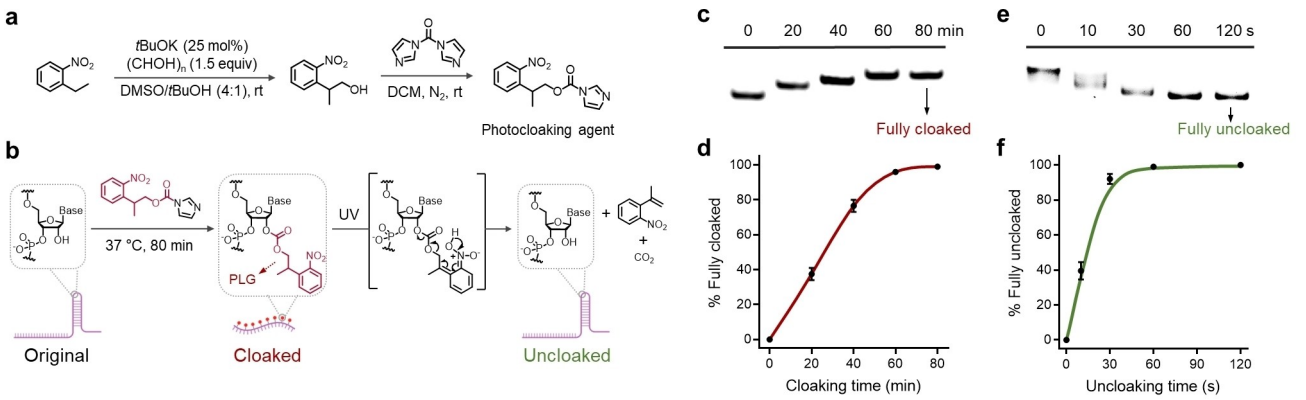


Figure 1. One-step cloaking and photo-induced uncloaking of crRNA. a) Synthetic route of the photocloaking agent. b) Schematic and mechanism of the acylation strategy; acylation of 2′-OH groups on crRNA strand with PLGs destroys crRNA structure and function, whereas 365 nm UV light irradiation (123 mW/cm^2) removes these PLGs. Illustration was created with BioRender.com. c) PAGE image of one-step cloaking of crRNA. The crRNA was treated with photocloaking agent at 37 °C for various acylation durations (20, 40, 60, and 80 min), followed by 20% PAGE analysis. d) The cloaking degree at the indicated time points. The data represents mean ($n=2$) normalized percentages versus band intensity of the original crRNA control. e) PAGE image of photo-induced uncloaking of crRNA. The fully cloaked crRNA was exposure to 365 nm UV light irradiation with various irradiation durations (0, 10, 30, 60, 90, and 120 s), followed by 20% PAGE analysis. f) The uncloaking degree at the indicated time points. The data represents mean ($n=2$) normalized percentages versus band intensity of the fully cloaked crRNA control.

on crRNA strand, and the crRNA strand was fully cloaked after 60 min (Figure 1c and d). Additionally, the results of mass spectrometry for original and fully cloaked crRNA also indicated the successful crRNA acylation (Figure S3 and S4). To assess the specificity of acylation reaction to RNA strand, a random DNA strand was employed, and the results indicated that no acylation reaction occurred on the DNA strand (Figure S5). With fully cloaked crRNA in hand, we wondered whether light irradiation can drive the removal of PLG adducts and recover the crRNA. To test this, we irradiated the fully cloaked crRNA with a 365 nm ultraviolet (UV) lamp (high-performance UV transilluminator, 123 mW/cm^2), and analyzed by PAGE. As shown in Figure 1e, with the extending irradiation time, the bands of cloaked crRNA returned to the band consistent with the migration of original crRNA. As a control, light irradiation did not affect the movement of original crRNA (Figure S6), suggesting that the migration of cloaked crRNA does attribute to the removal of PLG adducts upon exposure to light irradiation. Additionally, it could be observed that a short irradiation time (~1 min) was sufficient to remove PLG adducts (Figure 1f). Based on the above results, we can conclude that the crRNA can be temporarily cloaked by attaching PLG adducts on 2′-OH group, and subsequently restored after light irradiation. Additionally, we were very interested in whether the 2′-OH acylation strategy is universal and accessible to other crRNAs with diversified spacer regions. As shown in Figure S7 and S8, the PAGE results were greatly consistent with the observation of successful cloaking and photo-induced uncloaking of crRNAs, manifesting the versatility of the acylation strategy for photo-controlled crRNAs. Additionally, it was also observed the successful and simultaneous cloaking/uncloaking of various crRNAs (crRNA1~crRNA3) in single tube (Figure S9). We next explored the possibility of spontaneous uncloaking of the cloaked crRNA under ambient environment. To this end, a long time-course experiment was implemented, and no spontaneous uncloaking occurred even over 4 h (Figure S10), which was a long enough period of time to complete nucleic acid amplification, indicating that the cloaked crRNA was quite stable under ambient light exposure.

Effect of Cloaking and Photo-Induced Uncloaking of crRNA on the CRISPR–Cas12a System

The eminent acylation and effective photo-induced deacylation of crRNA make it possible to control the activity of CRISPR–Cas12a system. The Cas12a protein belongs to a type V-A CRISPR DNase,[52] which has been repurposed as a powerful tool for nucleic acid detection. A prominent property of CRISPR–Cas12a system is that the Cas12a can induce site-specific *cis*-cleavage of target double-stranded or single-stranded DNA (dsDNA or ssDNA) after recognition,[13] followed by *trans*-cleavage of non-specific ssDNA substrates, which allows us to fully investigate the effect of cloaking and photo-induced uncloaking of crRNA on CRISPR–Cas12a system (Figure 2a). As an initial assessment of whether the cloaked crRNA can inhibit *cis*- and *trans*-cleavage activities of Cas12a, we performed PAGE and fluorescence kinetic analysis. To this end, the Cas12a from *Lachnospiraceae bacterium* ND2006 Cas12a (LbCas12a) and crRNAs with different acylation time were employed. As shown in Figure 2b, we observed that the cleaved products by the Cas12a coupling with cloaked crRNA were gradually decreased with the increase of acylation time, indicating the acylation-induced *cis*-cleavage inhibition. Subsequently, we examined the effect of cloaked crRNA on the trans-cleavage activity of CRISPR–Cas12a system. In this study, a ssDNA substrate labelled with a fluorophore and quencher pair at each end (termed FQ-

© 2024 Wiley-VCH GmbH

15213773, 2024, 23, Downloaded from https://onlinelibrary.wiley.com/doi/10.1002/anie.202401486 by Shanghai Normal University, Wiley Online Library on [09/04/2025]. See the Terms and Conditions (https://onlinelibrary.wiley.com/terms-and-conditions) on Wiley Online Library for rules of use; OA articles are governed by the applicable Creative Commons License

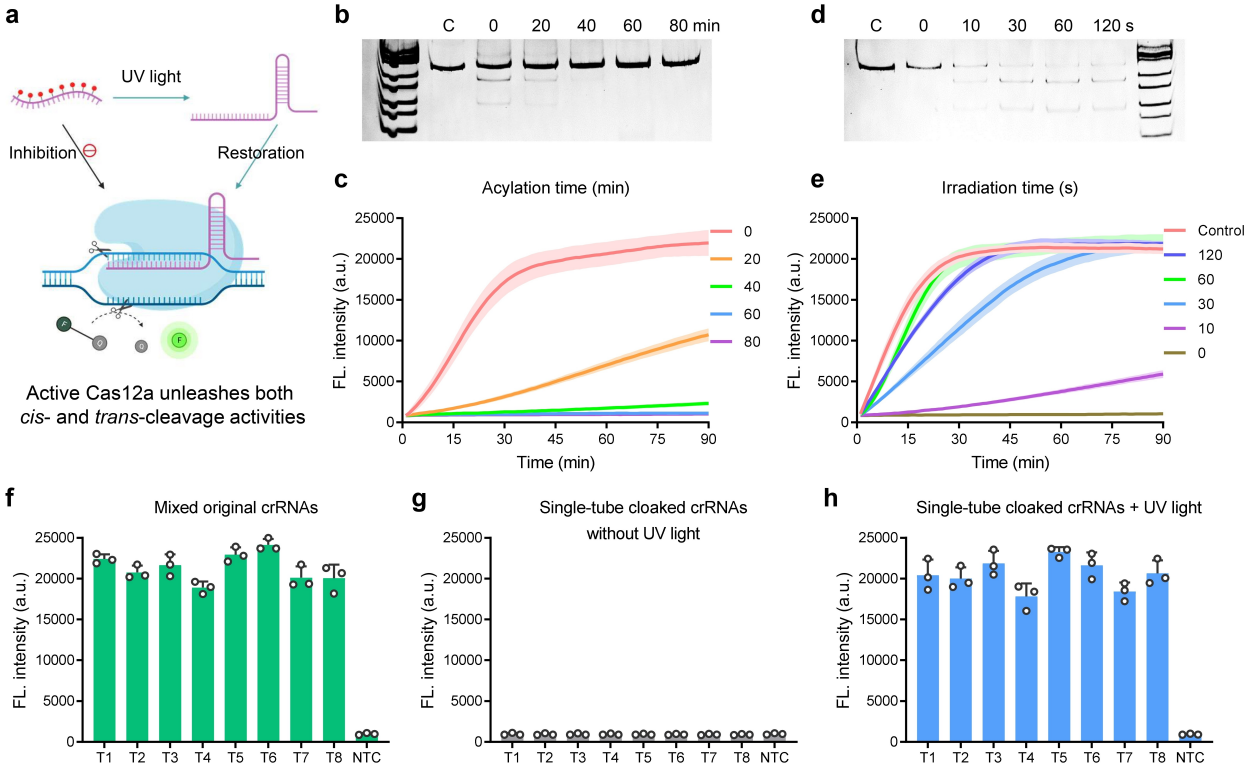


Figure 2. Effect of cloaking and photo-induced uncloaking of crRNA on the CRISPR–Cas12a system. a) crRNA cloaking inhibited the activity of CRISPR–Cas12a system, while photo-induced uncloaking of crRNA reinstated the activity of CRISPR–Cas12a system. Illustration was created with BioRender.com. b) PAGE analysis of the cloaking of crRNA inhibiting the CRISPR–Cas12a *cis*-cleavage activity. Original crRNAs were acylated at 37 °C with a gradually increasing time up to 80 min and coupled with Cas12a and *cis* template DNA, followed by 12% PAGE analysis. The control experiment (termed C) represents the *cis* template DNA only. c) Fluorescence kinetic analysis of cloaked crRNA inhibiting the CRISPR–Cas12a *trans*-cleavage activity. Original crRNAs were acylated with different time. d) PAGE analysis of photo-induced uncloaking of crRNA reinstating the CRISPR–Cas12a *cis*-cleavage activity. Fully cloaked crRNAs were irradiated by 365 nm UV light with a gradually increasing time and coupled with Cas12a and *cis* template DNA, followed by 12% PAGE analysis. The control experiment (termed C) represents the *cis* template DNA only. e) Fluorescence kinetic analysis of photo-induced uncloaking of crRNA reinstating the CRISPR–Cas12a *trans*-cleavage activity. Fully cloaked crRNAs experienced different irradiation time. f–h) Investigation of the universality of photo-induced reinstation of CRISPR–Cas12a activity using simultaneously acylated crRNAs with different spacer regions in a single tube. "T" stands for target DNA. These different crRNAs were acylated at 37 °C for 80 min, followed by 365 nm UV light irradiation for 60 s in the presence of their own target DNA. The fluorescence intensities of mixed original crRNAs (f), single-tube cloaked crRNAs (g), single-tube photo-induced uncloaked crRNAs (h). The PAGE analysis was conducted in duplicate, while the fluorescence experiments were performed in triplicate and data was represented by mean ± standard deviation.

reporter) was used to facilitate the analysis. The results indicated that the acylation of crRNA also made a significant inhibition effect on *trans*-cleavage activity of CRISPR–Cas12a system (Figure 2c). Thus, we concluded that the crRNA acylation could effectively suppress the CRISPR–Cas12a activity, and there was a direct relationship between the cloaking extent of crRNA and inhibition extent of Cas12a activity. We then expected to determine how many PLG adducts were required for complete inactivation of crRNA. In theory, the ribose 2′-OH acylation with one PLG adduct will result in a 208 Da molecular weight increment. Therefore, for fully cloaked crRNA, about 12 PLG adducts were calculated from the mass spectrometry results (Figure S4), suggesting that 12 PLG adducts were sufficient to completely inactive crRNA.

Encouraged by the above results, we next assessed whether the Cas12a coupling with cloaked crRNA would show reinstated activity under light irradiation. As expected, being consistent with the above photo-induced uncloaking assay (Figure 1d), we determined that 365 nm UV light irradiation was effective in restoring the *cis*-cleavage activity of CRISPR–Cas12a system. As shown in Figure 2d, site-specific cleavage of target dsDNA was observed to be dependent on the crRNA recovery under light irradiation. We then tested the effect of photo-induced uncloaking of crRNA on the *trans*-cleavage activity of CRISPR–Cas12a system. The results showed that the *trans*-cleavage activity gradually recovered with the prolonging light irradiation time (Figure 2e), and 60 s light irradiation was sufficient to reinstate the CRISPR–Cas12a activity. Additionally, it was observed that the *trans*-cleavage activity of CRISPR–Cas12a system declined slightly with a longer irradiation time. We thus evaluated the effect of irradiation time on CRISPR components including crRNA and Cas12a effector. The results showed that the long-time irradiation has a greater impact on Cas12a effector than crRNA (Figure S11). Next, to elucidate the universality and accessibility of the photo-induced restoration of CRISPR–Cas12a activity, another

© 2024 Wiley-VCH GmbH

15213773, 2024, 23, Downloaded from https://onlinelibrary.wiley.com/doi/10.1002/anie.202401486 by Shanghai Normal University, Wiley Online Library on [09/04/2025]. See the Terms and Conditions (https://onlinelibrary.wiley.com/terms-and-conditions) on Wiley Online Library for rules of use; OA articles are governed by the applicable Creative Commons License

seven original crRNAs with different spacer regions were experienced individually one-step acylation reaction, followed by evaluation using fluorescence kinetic analysis. Similar inhibition and restoration effect on CRISPR–Cas12a activity were observed when using the above individually cloaked crRNAs (Figure S12). As a further assessment, we attempted to simultaneously acylate these 8 original crRNAs (crRNA1~crRNA8, Table S1) in single tube and evaluated their property in the photo-initiated CRISPR–Cas12a activity. As expected, inconspicuous fluorescence signal could be seen for single-tube cloaked crRNAs even in the presence of their own target DNA, whereas light irradiation induced remarkable signal restoration, which was comparable to that of 8 mixed original crRNAs (Figure 2f–h).

Having completed the evaluation of the effects of cloaking and photo-induced uncloaking of crRNA on the CRISPR–Cas12a activity, we then investigated the potential inactivation mechanism by which the cloaked crRNA inhibits CRISPR–Cas12a activity. Previous literatures have demonstrated that the RNA acylation could disrupt its original conformation so as to decrease its affinity to target protein.[43,47] And another work confirmed that chemical cloaking of crRNA significantly decreased the interaction between cloaked crRNA and Cas protein.[53] While in the CRISPR–Cas12a system, crRNA can be considered as an aptamer toward Cas12a, thus the cloaked crRNA may disrupt its own conformation, affecting the binding affinity to Cas12a. In this study, we mainly examined whether the cloaked crRNA would affect its hybridization with target DNA. To this end, the original and cloaked crRNAs were incubated separately with their complementary DNA strand, and subsequently analyzed by PAGE. As shown in Figure S13, it was very inefficient to form heteroduplexes between the cloaked crRNA and its complementary DNA (lane 5), but a strong recovery of hybridization could be observed after light irradiation (lane 6). The UV melting study was also performed to investigate the interaction between cloaked crRNA and its complementary DNA. The melting curves showed that the 2′-OH acylation of crRNA with PLGs significantly reduced the Watson–Crick base pairs in cloaked crRNA and its complementary DNA, and melting temperature of the cloaked crRNA showed a ~11 °C drop than that of original crRNA (Figure S14). These results suggested that crRNA acylation strongly impaired the hybridization capacity between crRNA and its complementary DNA strand. Taken together, the inactivation mechanism can be attributed to the disrupted crRNA conformation, Cas12a–crRNA binding, as well as crRNA-target DNA hybridization.

POIROT for SARS-CoV-2 RNA Assay

Having investigated the effectiveness of the acylation strategy in controlling CRISPR–Cas12a activity, we next became interested in establishing a photo-initiated one-pot CRISPR testing (POIROT) (Figure 3a). Prior to that, we focused on evaluating the nucleic acid detection performance of photo-initiated CRISPR–Cas12a system. And the Cas12a coupling with original crRNA was served as the control. We observed a similar detection performance toward synthetic target DNA for both original and photo-induced uncloaked crRNAs (Figure 3b–d). As a follow evaluation of how light affects POIROT, we implemented component removal experiment. To this end, RPA, a frequently-used isothermal nucleic acid amplification technology, was employed to generate amplificons for subsequent CRISPR reaction. We found that no fluorescence signal was generated without UV light, even when all the required components were added. However, a considerable fluorescence signal produced after light irradiation (Figure 3e), suggestive of the light-dependent character of the designed POIROT.

We next attempted to constructed POIROT for the detection of severe acute respiratory syndrome coronavirus 2 (SARS-CoV-2) RNA standards by combining with reverse transcription-RPA (RT-RPA) reaction. First, we explored the differences in the detection performance of two-step assay, conventional one-step assay, and POIROT using original crRNA (two-step and conventional one-step assay) and cloaked crRNA (POIROT), respectively, for the detection of nucleocapsid protein gene (N gene) of SARS-CoV-2. As shown in Figure 3f–i, we found that POIROT exhibited excellent analytical capability comparable to two-step assay with a detectable limit of 1 copy/μL. However, the conventional one-step assay could only effectively detect 100 copies/μL N gene, which is almost two orders of magnitude lower than POIROT. In addition, similar results were obtained when using the three methods for the detection of open reading frame 1ab gene (O gene) of SARS-CoV-2 (Figure 3j, Figure S15). In the above experiments, the nucleic acid amplification was performed for 30 min and then exposed to light irradiation. We considered whether the amplification time has an impact on the detection efficiency of POIROT. We thus set a short amplification time, such as 10 or 20 min. Surprisingly, POIROT showed the same detectable limit regardless of the amplification time (Figure S16).

Clinical Application of POIROT for HPV-16 and HPV-18 Diagnostics

Having achieved robust one-pot SARS-CoV-2 RNA assay using POIROT, we then assessed the platform for human papilloma virus (HPV) DNA assay (Figure 4a). Studies have shown a strong relationship between persistent high-risk HPV infection and cervical cancer development, especially types HPV-16 and HPV-18.[54] To this end, we first performed POIROT to detect various concentrations of HPV-16 and HPV-18 DNA standards, respectively. As shown in Figure 4a and b, POIROT could reliably detect as low as 1 copy/μL of HPV-16 and HPV-18 DNA standards under 30 min amplification time. Before analyzing clinical HPV-16 and HPV-18 samples, we explored the specificity of POIROT through testing and comparing other HPV subtypes (such as HPV-33, HPV-39, HPV-51, HPV-52, HPV-56, HPV-58, HPV-66, and HPV-68). The results showed that

© 2024 Wiley-VCH GmbH

15213773, 2024, 23, Downloaded from https://onlinelibrary.wiley.com/doi/10.1002/anie.202401486 by Shanghai Normal University, Wiley Online Library on [09/04/2025]. See the Terms and Conditions (https://onlinelibrary.wiley.com/terms-and-conditions) on Wiley Online Library for rules of use; OA articles are governed by the applicable Creative Commons License

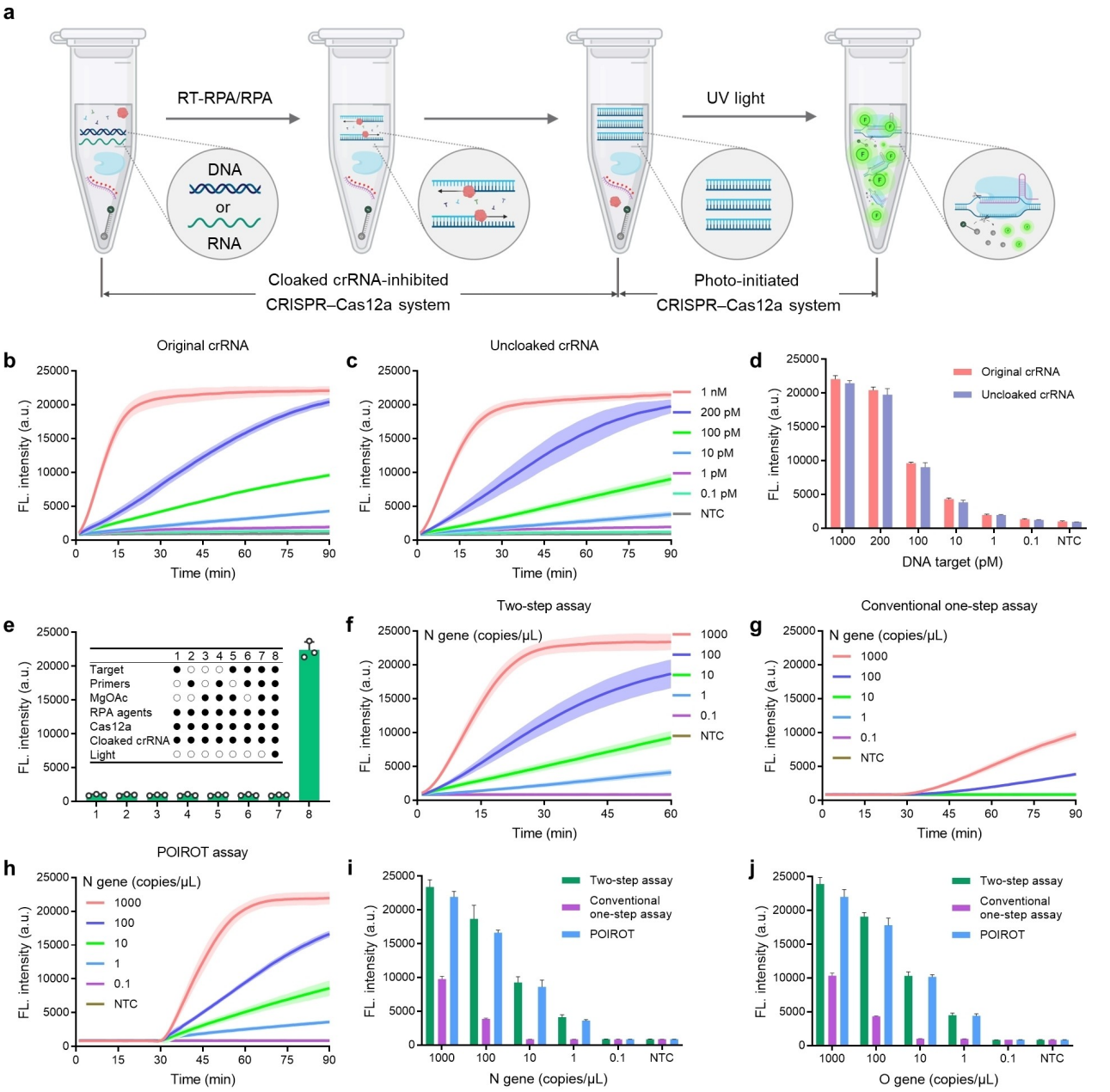


Figure 3. Development of POIROT for nucleic acid detection. a) The schematic illustration of POIROT platform. POIROT integrated RT-RPA or RPA and photo-initiated CRISPR–Cas12a system for nucleic acid detection. In the POIROT, RT-RPA/RPA is executed to obtain DNA amplicons, followed with photo-initiated CRISPR–Cas12a system for nucleic acid assay. Illustration was created with BioRender.com. b) Sensitivity analysis of the CRISPR–Cas12a system using original crRNA with different target DNA concentrations. c) Sensitivity analysis of the CRISPR–Cas12a system using photo-induced uncloaked crRNA with different target DNA concentrations. d) Comparison of the fluorescence intensity of CRISPR–Cas12a system using original and photo-induced uncloaked crRNAs. e) Component removal experiments to certify the POIROT concept. In this assay, N gene-targeted crRNA was used for SARS-CoV-2 RNA detection. f)–i) Sensitivity analysis for N gene of SARS-CoV-2 RNA standards detection using two-step assay (f), conventional one-step assay (g), and our POIROT assay (h), and their corresponding endpoint fluorescence intensity (i). j) Endpoint fluorescence intensity of O gene of SARS-CoV-2 RNA standards detection using two-step assay, conventional one-step assay, and our POIROT assay. These experiments were performed in triplicate and data was represented by mean ± standard deviation.

only HPV-16 and HPV-18 induced significant fluorescence signals in the presence of their corresponding crRNA, while other HPV subtypes could not generate increased signals, indicating excellent analytical specificity of POIROT (Figure 4c).

Finally, we explored the practicability of POIROT through analyzing a total of 150 clinical vaginal swab samples including 100 suspected HPV-16 and 50 suspected HPV-18 samples (Figure 4d). These clinical samples were first confirmed by qPCR method. Using a cycle threshold (C_t) value of 40 as the judgement criterion, the qPCR results

© 2024 Wiley-VCH GmbH

15213773, 2024, 23, Downloaded from https://onlinelibrary.wiley.com/doi/10.1002/anie.202401486 by Shanghai Normal University, Wiley Online Library on [09/04/2025]. See the Terms and Conditions (https://onlinelibrary.wiley.com/terms-and-conditions) on Wiley Online Library for rules of use; OA articles are governed by the applicable Creative Commons License

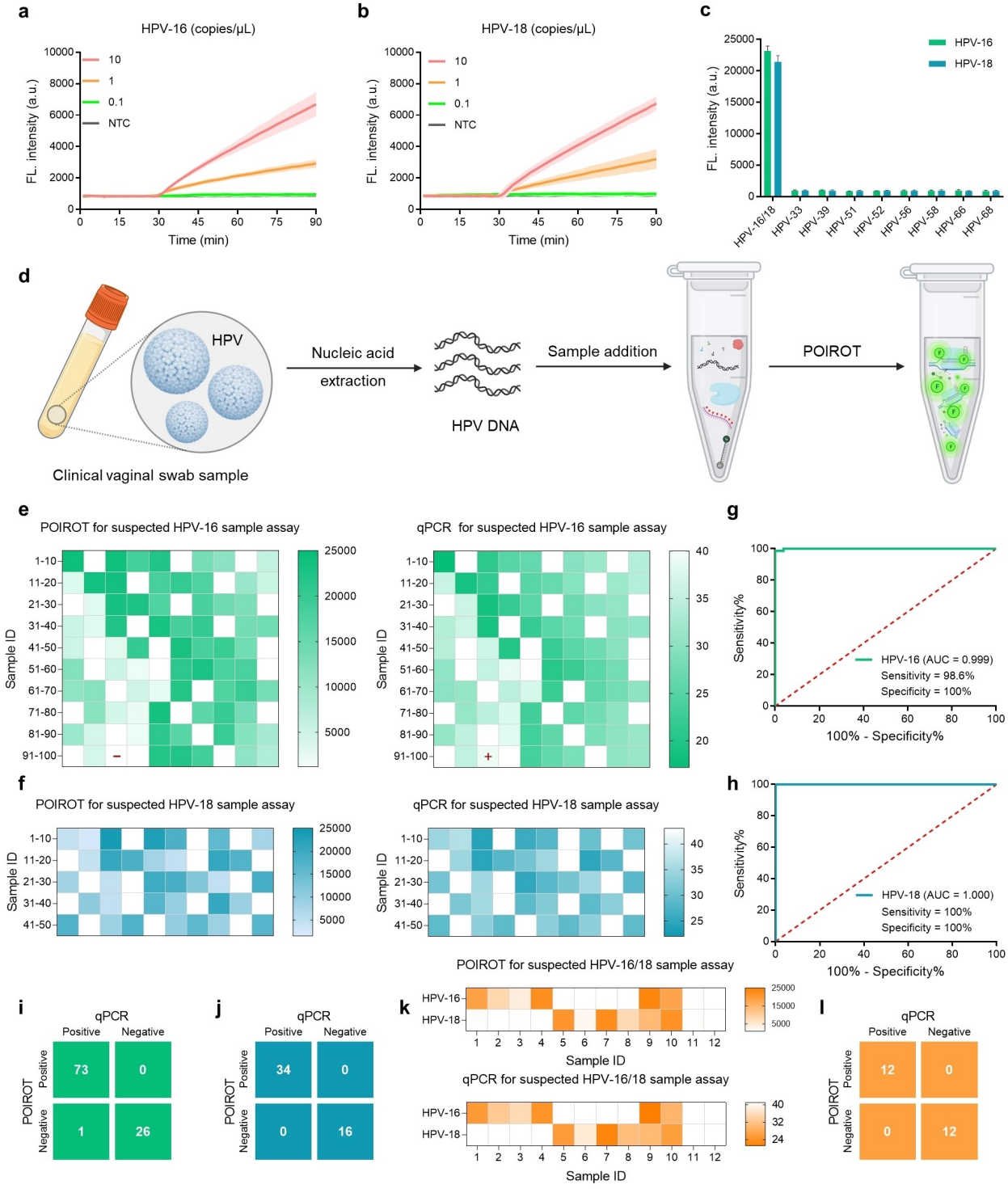


Figure 4. Clinical application of POIROT for HPV-16 and HPV-18 assays. a) Analysis of HPV-16 DNA standards by POIROT. b) Analysis of HPV-18 DNA standards by POIROT. c) Schematic illustration of HPV assay in human vaginal swab samples. d) Specificity analysis of POIROT using other HPV subtypes. These above experiments were performed in triplicate and data was represented by mean ± standard deviation. e) Clinical HPV-16 sample assay by POIROT, which are confirmed by qPCR. The heat map represents the fluorescence intensities (left panel) and C_t values (right panel) of each sample. The one suspected HPV-16 sample that was failure to be detected, is labeled with "−" in the left panel and "+" in the right panel, respectively. f) Clinical HPV-18 sample assay by POIROT, which are confirmed by qPCR. The heat map represents the fluorescence intensities (left panel) and C_t values (right panel) of each sample. g), h) ROC curve analysis of POIROT detection accuracy in clinical applications. i), j) Confusion matrix summarizing the assay discrimination performance between positive and negative clinical samples by POIROT and qPCR. k) Clinical HPV-16/18 sample assay by POIROT using simultaneously acylated crRNAs, which are confirmed by qPCR. The heat map represents the fluorescence intensities (upper panel) and C_t values (lower panel) of each sample. l) Confusion matrix summarizing the assay discrimination performance between positive and negative clinical samples by POIROT and qPCR.

© 2024 Wiley-VCH GmbH

15213773, 2024, 23, Downloaded from https://onlinelibrary.wiley.com/doi/10.1002/anie.202401486 by Shanghai Normal University, Wiley Online Library on [09/04/2025]. See the Terms and Conditions (https://onlinelibrary.wiley.com/terms-and-conditions) on Wiley Online Library for rules of use; OA articles are governed by the applicable Creative Commons License

indicated that there were 74 HPV-16 positive samples, 26 HPV-16 negative samples, 34 HPV-18 positive samples, and 16 HPV-18 negative samples (Figure S17–S22, Table S2 and S3). Subsequently, the practicability of POIROT was assessed using these qPCR-confirmed clinical samples (Figure 4e and f, Figure S23–S25). The testing results were in good agreement with qPCR analysis (Figure 4e–h), except for one suspected HPV-16 sample ($C_t = 39.91$) that was failure to be detected (Figure 4e). Based on the above results, we obtained a corresponding receiver operating characteristic (ROC) curve of the clinical sample assay (Figure 4g–j), which showed excellent sensitivity and specificity for the detection of HPV-16 (98.6 % and 100 %) and HPV-18 (100 % and 100 %), respectively.

Furthermore, to evaluate the clinical application of simultaneously acylated crRNAs in single tube, the simultaneously acylated HPV-16/18-crRNAs in single tube were utilized to test additional 12 qPCR-conformed clinical samples including 4 HPV-16 positive samples, 4 HPV-18 positive samples, and 2 HPV-16/18 co-positive samples, as well as 2 HPV-16/18 co-negative samples (Figure S26, Table S4). The results of POIROT assay were greatly consistent with qPCR analysis, verifying that these simultaneously acylated crRNAs based on the universal acylation strategy could also be applied in clinical sample detection (Figure 4k and l, Figure S27).

After having demonstrated that POIROT has comparable sensitivity and specificity to qPCR, and the detection efficiency of POIROT could be still maintained in a short amplification time (10 or 20 min) (Figure S16). We then investigated whether POIROT can identify clinical HPV-positive samples under a shortened amplification time. To this end, we measured five samples with different C_t values (<36) using POIROT and qPCR, respectively. The results showed that our POIROT could distinguish these positive samples within 20 min, while a longer time (>35 min) was required for qPCR method, suggesting a faster detection speed of POIROT than qPCR (Figure S28). Taken together, it is anticipated that POIROT hold great potential in the robust and rapid clinical diagnostics of infectious diseases.

Conclusion

Exploring rapid, sensitive, and high-efficiency nucleic acid detection approaches is essential to clinical diagnosis and biomedical research. Currently, qPCR is the gold-standard technique of nucleic acid assay with merits of versatility, robustness and sensitivity, which is the most commonly adopted for the detection of nucleic acid biomarkers in central laboratories. However, due to the need for a thermocycling process, it is time-consuming and is not conducive to large-scale nucleic acid screening. Although isothermal amplification technologies circumvent the requirement of thermal cyclers, their sensitivity and specificity are often difficult to match that of qPCR. The existing CRISPR technology holds great potential in overcoming these obstacles to develop rapid, accurate, and high-efficiency molecular diagnosis due to its precise RNA-guided nucleic acid recognition and robust *trans*-cleavage-mediated signal amplification abilities (CRISPR–Cas12 and CRISPR–Cas13 systems). Based on these unique properties, several nucleic acid detection strategies coupling with isothermal amplification, such as DETECTR,[13] and SHERLOCK,[17] platforms, have been developed. In these strategies, nucleic acid amplification and CRISPR reaction need to be separately conducted, which not only involves complicated operation procedure, but also has the risk of aerosol contamination.[18–20] However, if the isothermal amplification reaction is carried out in the same tube as the CRISPR system, the *cis*- and *trans*-cleavage will destruct the isothermal amplification templates and primers to a certain extent, respectively, thus affecting the amplification efficiency and detection sensitivity. Although some reformative one-step CRISPR researches have been reported, these methods are still inconvenient, or sacrifice the efficacy of the CRISPR reaction.[19,24–29] To address this issue, the photo-controlled one-pot assays were developed and exhibited some advantages, but they still are rather cumbersome and need trial-and-error screening. Therefore, a universal strategy that does not perform permutation and combination screening of modifications, regardless of target sequences, but can rapidly reinstate the activity of CRISPR system upon exposure to light irradiation, is still desirable for photo-controlled one-pot CRISPR assay.

In this work, we developed a universal and accessible acylation strategy for the fabrication of photoresponsive cloaked crRNA to realize the photo-initiated CRISPR–Cas12a activity. Our results showed that the crRNA function was temporarily suspended by attaching PLGs on 2′-OH groups, and subsequently restored by 1 min light irradiation, regardless of the crRNA sequence, which can bring great advantages and convenience for crRNA design and synthesis when the target changes (Table S5). In addition, we investigated the potential inactivation mechanisms by which cloaked crRNA suppressed the CRISPR–Cas12a activity. The attached PLGs can prevent the effective hybridization between cloaked crRNA and its target DNA, and they may also decrease the binding affinity of cloaked crRNA to Cas12a enzyme due to the disturbed crRNA conformation. After achieving photo-initiated CRISPR–Cas12a reaction, we developed a universal POIROT (PhotO-Initiated CRISPR–Cas12a system for Robust One-pot Testing) integrating with RT-RPA/RPA reaction for SARS-CoV-2 RNA and HPV DNA detection. Since the isothermal amplification reaction is not affected by the CRISPR–Cas12a system, POIROT exhibited nearly two orders of magnitude more sensitive than the conventional one-step assay and was comparable to the two-step assay. In particular, compared to the gold-standard qPCR, POIROT showed relatively high sensitivity and specificity in the detection of clinical HPV samples. Additionally, due to the universality of acylation strategy, it is easy to obtain acylated crRNA for other targets detection regardless of its sequence and extend to other CRISPR systems including CRISPR–Cas13 and Cas14 systems[55–57] for establishing one-pot CRISPR assay. More importantly, given the fact that longer wavelength optical control is more suitable for applications in clinical diagnosis

© 2024 Wiley-VCH GmbH

15213773, 2024, 23, Downloaded from https://onlinelibrary.wiley.com/doi/10.1002/anie.202401486 by Shanghai Normal University, Wiley Online Library on [09/04/2025]. See the Terms and Conditions (https://onlinelibrary.wiley.com/terms-and-conditions) on Wiley Online Library for rules of use; OA articles are governed by the applicable Creative Commons License

and biomedical researches, we anticipate that the introduction of visible, infrared or even near-infrared responsive PLGs[30] on crRNA strand using the universal acylation strategy will be feasible and flexible for CRISPR activity regulation. However, it is worth noting that the types of PLGs (different chemical structures), their modified positions (2′-OH, nucleotide base, or phosphate group), and the synthesis methods of cloaked crRNA (solid-phase or post-modification synthesis) may affect the restoration efficiency of CRISPR activity, which will in turn impact the capability of CRISPR system for molecular diagnosis. Moreover, the specific experimental parameters of the detection system will also affect the analytical performance of the one-pot CRISPR assay. Generally, we believe this proposed approach will contribute to develop universal and accessible photo-controlled CRISPR technologies for one-pot assay, and even expand applications in controllable CRISPR-based genomic editing, disease therapy, and cell imaging.

Acknowledgements

This work was supported by the National Natural Science Foundation of China (22274046, 22334005), the Science and Technology Innovation Program of Hunan Province (2022RC1114), Hunan Provincial Innovation Foundation for Postgraduate (CX20220455).

Conflict of Interest

The authors declare no conflict of interest.

Data Availability Statement

The data that support the findings of this study are available from the corresponding author upon reasonable request.

Keywords: RNA acylation · Cloaked crRNA · Photo-initiated CRISPR–Cas12a · One-pot assay · Nucleic acid detection

[1] K. S. Makarova, D. H. Haft, R. Barrangou, S. J. Brouns, E. Charpentier, P. Horvath, S. Moineau, F. J. Mojica, Y. I. Wolf, A. F. Yakunin, J. van der Oost, E. V. Koonin, *Nat. Rev. Microbiol.* **2011**, *9*, 467–477.
[2] F. Hille, H. Richter, S. P. Wong, M. Bratovič, S. Ressel, E. Charpentier, *Cell* **2018**, *172*, 1239–1259.
[3] G. J. Knott, J. A. Doudna, *Science* **2018**, *361*, 866–869.
[4] M. Adli, *Nat. Commun.* **2018**, *9*, 1911.
[5] H. Wang, M. Nakamura, T. R. Abbott, D. Zhao, K. Luo, C. Yu, C. M. Nguyen, A. Lo, T. P. Daley, M. La Russa, Y. Liu, L. S. Qi, *Science* **2019**, *365*, 1301–1305.
[6] Y. Li, Y. Wu, R. Xu, J. Guo, F. Quan, Y. Zhang, D. Huang, Y. Pei, H. Gao, W. Liu, J. Liu, Z. Zhang, R. Deng, J. Shi, K. Zhang, *Nat. Commun.* **2023**, *14*, 7722.
[7] R. U. Sheth, S. S. Yim, F. L. Wu, H. H. Wang, *Science* **2017**, *358*, 1457–1461.
[8] D. S. Chertow, *Science* **2018**, *360*, 381–382.
[9] M. M. Kaminski, O. O. Abudayyeh, J. S. Gootenberg, F. Zhang, J. J. Collins, *Nat. Biomed. Eng.* **2021**, *5*, 643–656.
[10] Y. Tang, T. Song, L. Gao, S. Yin, M. Ma, Y. Tan, L. Wu, Y. Yang, Y. Wang, T. Lin, F. Li, *Nat. Commun.* **2022**, *13*, 4667.
[11] K. Shi, S. Xie, R. Tian, S. Wang, Q. Lu, D. Gao, C. Lei, H. Zhu, Z. Nie, *Sci. Adv.* **2021**, *7*, eabc7802.
[12] O. O. Abudayyeh, J. S. Gootenberg, S. Konermann, J. Joung, I. M. Slaymaker, D. B. Cox, S. Shmakov, K. S. Makarova, E. Semenova, L. Minakhin, K. Severinov, A. Regev, E. S. Lander, E. V. Koonin, F. Zhang, *Science* **2016**, *353*, aaf5573.
[13] J. S. Chen, E. Ma, L. B. Harrington, M. Da Costa, X. Tian, J. M. Palefsky, J. A. Doudna, *Science* **2018**, *360*, 436–439.
[14] S. Y. Li, Q. X. Cheng, J. K. Liu, X. Q. Nie, G. P. Zhao, J. Wang, *Cell Res.* **2018**, *28*, 491–493.
[15] Y. Dai, Y. Wu, G. Liu, J. J. Gooding, *Angew. Chem. Int. Ed.* **2020**, *59*, 20754–20766.
[16] S. Y. Li, Q. X. Cheng, J. M. Wang, X. Y. Li, Z. L. Zhang, S. Gao, R. B. Cao, G. P. Zhao, J. Wang, *Cell Discov.* **2018**, *4*, 20.
[17] J. S. Gootenberg, O. O. Abudayyeh, J. W. Lee, P. Essletzbichler, A. J. Dy, J. Joung, V. Verdine, N. Donghia, N. M. Daringer, C. A. Freije, C. Myhrvold, R. P. Bhattacharyya, J. Livny, A. Regev, E. V. Koonin, D. T. Hung, P. C. Sabeti, J. J. Collins, F. Zhang, *Science* **2017**, *356*, 438–442.
[18] X. Ding, K. Yin, Z. Li, R. V. Lalla, E. Ballesteros, M. M. Sfeir, C. Liu, *Nat. Commun.* **2020**, *11*, 4711.
[19] S. Lu, X. Tong, Y. Han, K. Zhang, Y. Zhang, Q. Chen, J. Duan, X. Lei, M. Huang, Y. Qiu, D.-Y. Zhang, X. Zhou, Y. Zhang, H. Yin, *Nat. Biomed. Eng.* **2022**, *6*, 286–297.
[20] H. Yan, Y. Wen, Z. Tian, N. Hart, S. Han, S. J. Hughes, Y. Zeng, *Nat. Biomed. Eng.* **2023**, *7*, 1583–1601.
[21] F. Shao, J. S. Park, J. S. Park, G. Zhao, K. Hsieh, T. H. Wang, *Anal. Chem.* **2023**, *95*, 3873–3882.
[22] J. Joung, A. Ladha, M. Saito, N. G. Kim, A. E. Woolley, M. Segel, R. P. J. Barretto, A. Ranu, R. K. Macrae, G. Faure, E. I. Ioannidi, R. N. Krajeski, R. Bruneau, M. L. W. Huang, X. G. Yu, J. Z. Li, B. D. Walker, D. T. Hung, A. L. Greninger, K. R. Jerome, J. S. Gootenberg, O. O. Abudayyeh, F. Zhang, *N. Engl. J. Med.* **2020**, *383*, 1492–1494.
[23] J. Arizti-Sanz, C. A. Freije, A. C. Stanton, B. A. Petros, C. K. Boehm, S. Siddiqui, B. M. Shaw, G. Adams, T. F. KosokoThoroddsen, M. E. Kemball, J. N. Uwanibe, F. V. Ajogbasile, P. E. Eromon, R. Gross, L. Wronka, K. Caviness, L. E. Hensley, N. H. Bergman, B. L. MacInnis, C. T. Happi, J. E. Lemieux, P. C. Sabeti, C. Myhrvold, *Nat. Commun.* **2020**, *11*, 5921.
[24] Wang, J. Wu, J. Li, J. Wang, H. Liu, Y. Wang, *Anal. Chem.* **2019**, *91*, 12156–12161.
[25] L. Guo, X. Sun, X. Wang, C. Liang, H. Jiang, Q. Gao, M. Dai, B. Qu, S. Fang, Y. Mao, Y. Chen, G. Feng, Q. Gu, R. R. Wang, Q. Zhou, W. Li, *Cell Discov.* **2020**, *6*, 34.
[26] Y. Chen, Y. Mei, X. Zhao, X. Jiang, *Anal. Chem.* **2020**, *92*, 14846–14852.
[27] S. M. Xia, X. Chen, *Cell Discov.* **2020**, *6*, 37.
[28] K. Yin, X. Ding, Z. Li, H. Zhao, K. Cooper, C. Liu, *Anal. Chem.* **2020**, *92*, 8561–8568.
[29] M. Lin, H. Yue, T. Tian, E. Xiong, D. Zhu, Y. Jiang, X. Zhou, *Anal. Chem.* **2022**, *94*, 8277–8284.
[30] Q. Liu, A. Deiters, *Acc. Chem. Res.* **2014**, *47*, 45–55.
[31] Y. Nihongaki, F. Kawano, T. Nakajima, M. Sato, *Nat. Biotechnol.* **2015**, *33*, 755–760.
[32] J. Hemphill, E. K. Borchardt, K. Brown, A. Asokan, A. Deiters, *J. Am. Chem.* **2015**, *137*, 5642–5645.
[33] P. K. Jain, V. Ramanan, A. G. Schepers, N. S. Dalvie, A. Panda, H. E. Fleming, S. N. Bhatia, *Angew. Chem. Int. Ed.* **2016**, *55*, 12440–12444.
[34] Y. Liu, R. S. Zou, S. He, Y. Nihongaki, X. Li, S. Razavi, B. Wu, T. Ha, *Science* **2020**, *368*, 1265–1269.

© 2024 Wiley-VCH GmbH

15213773, 2024, 23, Downloaded from https://onlinelibrary.wiley.com/doi/10.1002/anie.202401486 by Shanghai Normal University, Wiley Online Library on [09/04/2025]. See the Terms and Conditions (https://onlinelibrary.wiley.com/terms-and-conditions) on Wiley Online Library for rules of use; OA articles are governed by the applicable Creative Commons License

[35] W. Zhou, W. Brown, A. Bardhan, M. Delaney, A. S. Ilk, R. R. Rauen, S. I. Kahn, M. Tsang, A. Deiters, *Angew. Chem. Int. Ed.* **2020**, *132*, 9083–9088.
[36] J. Carlson-Stevermer, R. Kelso, A. Kadina, S. Joshi, N. Rossi, J. Walker, R. Stoner, T. Maures, *Nat. Commun.* **2020**, *11*, 5041.
[37] M. Hu, Z. Qiu, Z. Bi, T. Tian, Y. Jiang, X. Zhou, *Proc. Natl. Acad. Sci. USA* **2022**, *119*, e2202034119.
[38] Y. Chen, X. Xu, J. Wang, Y. Zhang, W. Zeng, Y. Liu, X. Zhang, *Anal. Chem.* **2022**, *94*, 9724–9731.
[39] M. Hu, R. Liu, Z. Qiu, F. Cao, T. Tian, Y. Lu, Y. Jiang, X. Zhou, *Angew. Chem. Int. Ed.* **2023**, *62*, e202300663.
[40] Y. J. Sun, W. D. Chen, J. Liu, J. J. Li, Y. Zhang, W. Q. Cai, L. Liu, X. J. Tang, J. Hou, M. Wang, L. Cheng, *Angew. Chem. Int. Ed.* **2023**, *62*, e202212413.
[41] X. Fei, C. Lei, W. Ren, X. Liu, C. Liu, *Anal. Chem.* **2023**, *95*, 12169–12176.
[42] W. A. Velema, E. T. Kool, *Nat. Chem. Rev.* **2020**, *4*, 22–37.
[43] A. Kadina, A. M. Kietrys, E. T. Kool, *Angew. Chem. Int. Ed.* **2018**, *57*, 3059–3063.
[44] W. A. Velema, A. M. Kietrys, E. T. Kool, *J. Am. Chem. Soc.* **2018**, *140*, 3491–3495.
[45] L. Xiao, Y. W. Jun, E. T. Kool, *Angew. Chem. Int. Ed.* **2021**, *60*, 26798–26805.
[46] L. Fang, L. Xiao, Y. W. Jun, Y. Onishi, E. T. Kool, *Nat. Chem.* **2023**, *15*, 1296–1305.
[47] M. Habibian, C. McKinlay, T. R. Blake, A. M. Kietrys, R. M. Waymouth, P. A. Wendera, E. T. Kool, *Chem. Sci.* **2020**, *11*, 1011–1016.
[48] Y. Liu, Y. Shi, L. Yu, Z. Wu, J. H. Jiang, *Anal. Chem.* **2023**, *95*, 6490–6495.
[49] H. Lei, T. Zeng, X. Ye, R. Fan, W. Xiong, T. Tian, X. Zhou, *Adv. Sci.* **2023**,*10*, 2206433.
[50] H. Ji, W. Xiong, S. Guo, S. Wang, X. Xing, T. Tian, X. Zhou, *ACS Chem. Biol.* **2023**, *18*, 1829–1837.
[51] S. Wang, L. Wei, J. Q. Wang, H. Ji, W. Xiong, J. Liu, P. Yin, T. Tian, X. Zhou, *ACS Chem. Biol.* **2020**, *15*, 1455–1463.
[52] B. Zetsche, J. S. Gootenberg, O. O. Abudayyeh, I. M. Slaymaker, K. S. Makarova, P. Essletzbichler, S. E. Volz, J. Joung, J. van der Oost, A. Regev, E. V. Koonin, F. Zhang, *Cell* **2015**, *163*, 759–771.
[53] S. R. Wang, L. Y. Wu, H. Y. Huang, W. Xiong, J. Liu, L. Wei, P. Yin, T. Tian, X. Zhou, *Nat. Commun.* **2020**, *11*, 91.
[54] C. B. J. Woodman, S. I. Collins, L. S. Young, *Nat. Rev. Cancer* **2007**, *7*, 11–22.
[55] D. Chen, W. T. Huang, Y. Zhang, B. Chen, J. Tan, Q. Yuan, Y. B. Yang, *Angew. Chem. Int. Ed.* **2023**, *62*, e202304298.
[56] L. B. Harrington, D. Burstein, J. S. Chen, D. Paez-Espino, E. Ma, I. P. Witte, J. C. Cofsky, N. C. Kyrpides, J. F. Banfield, J. A. Doudna, *Science* **2018**, *362*, 839–842.
[57] Y. Wei, Z. Yang, C. Zong, B. Wang, X. Ge, X. Tan, X. Liu, Z. Tao, P. Wang, C. Ma, Y. Wan, J. Li, *Angew. Chem. Int. Ed.* **2021**, *60*, 24241–24247.

Manuscript received: January 22, 2024
Accepted manuscript online: April 2, 2024
Version of record online: April 30, 2024

© 2024 Wiley-VCH GmbH

15213773, 2024, 23, Downloaded from https://onlinelibrary.wiley.com/doi/10.1002/anie.202401486 by Shanghai Normal University, Wiley Online Library on [09/04/2025]. See the Terms and Conditions (https://onlinelibrary.wiley.com/terms-and-conditions) on Wiley Online Library for rules of use; OA articles are governed by the applicable Creative Commons License